Precise Facet Temperature Distribution of High- Power Laser Diodes: Unpumped Window Effect

Jérémy Michaud, Pamela del Vecchio, Laurent Béchou, David Veyrié, Mauro Bettiati, François Laruelle, Stéphane Grauby

Precise Facet Temperature Distribution of High-Power Laser Diodes: Unpumped Window Effect

Jérémy Michaud, Pamela Del Vecchio, Laurent Béchou, David Veyrié, Mauro Andrea Bettiati, Francois Laruelle, and Stéphane Grauby

***Abstract*— A thermoreflectance technique is used to evaluate the temperature variations at the output facet of high-power GaAs-based laser diodes emitting at 980 nm. Two kinds of diodes with different unpumped windows (UPWs) are studied to determine the influence of UPW length on the temperature variation. We show that in the vicinity of the active region, where a catastrophic optical damage is most susceptible to occur, the short UPW diode heats much more (up to 40%) than the long UPW one.**

***Index Terms*— Catastrophic optical degradation, facet temperature variation, laser diode, unpumped window.**

I. Introduction

FACET heating, mainly due to laser light absorption and surface carrier recombination, plays a major role concerning laser diode reliability [1]. The heating reduction, in particular near the active region, can increase the current threshold of catastrophic optical degradation (COD) and consequently the maximum output optical power. Introducing an unpumped window (UPW) architecture is one of the possible strategies to reduce the facet temperature and hence fabricate highly reliable devices with high power operation [2], [3]. The UPW consists in a region located at the diode front facet where current injection is reduced.

In this letter, we study 980nm emitting laser diodes which constitute performing systems in terms of output power, conversion efficiency and reliability. Two kinds of laser diodes are compared, considering either a short or a long UPW. Very few studies of the UPW impact on the facet temperature are reported in literature and most of them are simulations [4] or measurements of the ridge temperature [5]. μ-Raman facet measurements [6] can also be found but with large uncertainties and long acquisition times, which prevent this technique to be used for temperature mapping. Then, we use thermoreflectance (TR), which is a fast and very accurate technique, to compare the temperature variation for both structures in different locations of the output facet with a micrometric spatial resolution. Hence, for the first time, we can detail the influence of the UPW length on the temperature both far from the active region and close to it, where a COD is most likely to occur.

This work was supported by the Centre National d'Etudes Spatiales.

J. Michaud and S. Grauby are with the Université de Bordeaux, Laboratoire Ondes et Matière d'Aquitaine, Talence 33400, France (e-mail: jmichaud25@gmail.com; stephane.grauby@u-bordeaux.fr).

P. Del Vecchio, M. A. Bettiati, and F. Laruelle are with 3S Photonics, Nozay 91625, France (e-mail: pamela.delvecchio@ims-bordeaux.fr; mbettiati@3spgroup.com; flaruelle@3spgroup.com).

L. Béchou is with the Intégration du Matériau au Système, Université de Bordeaux, Talence 33405, France (e-mail: laurent.bechou@ims-bordeaux.fr).

D. Veyrié is with the Centre National d'Études Spatiales, Toulouse 31400, France (e-mail: david.veyrie@cnes.fr).

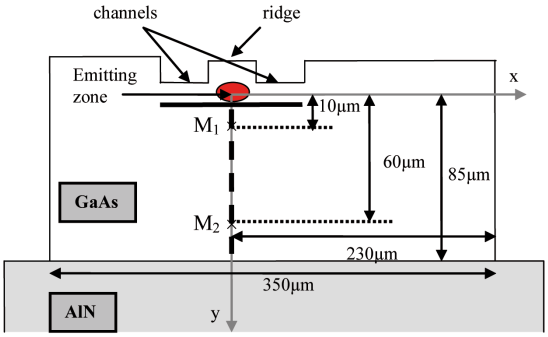

Fig. 1. Generic facet view of the laser diode.

II. Experimental Set Up and Devices Under Test

The devices under test (fig.1) are single AlGaAs/InGaAs quantum well laser diodes emitting at 980nm used for amplification in optical communication transmission systems [7]. The 3.9mm long ridge structure, covered by a gold layer, allows to confine the current and the light emission in the quantum well of the active region at the p-n junction.

We studied two kinds of devices, differing by their UPW length, either short (noted S-UPW) or long (noted L-UPW). The S-UPW is much smaller than the 30μm long UPW studied in [3] whereas the L-UPW has been lengthened with a diode power reduction limited to 1% at maximum. The diodes are biased using a ITC510 current source, to adjust the operating point, connected with a 33250A voltage generator to modulate the driving current which is a 50% duty cycle square current (f=442Hz) varying from 0.1mA to I_{max}; I_{max} can be adjusted from 6mA to 1A. This induces a temperature variation ΔT, hence a reflectivity relative variation $\Delta R/R$:

$$\frac{\Delta R}{R} = \frac{1}{R}\frac{\partial R}{\partial T}\Delta T = \kappa \Delta T \qquad (1)$$

where R is the sample mean reflectivity and κ is the thermoreflectance coefficient mainly depending on the nature

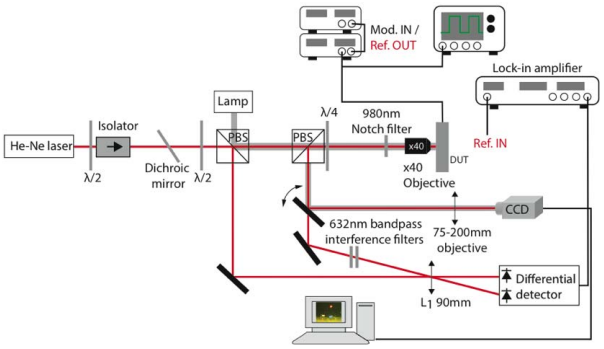

Fig. 2. Thermoreflectance set-up.

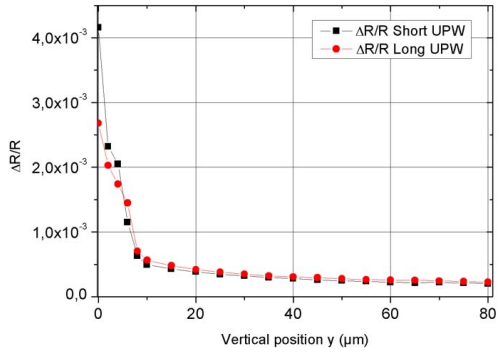

Fig. 3. ΔR/R signal along the vertical y-axis from source to base at 800mA.

of the material and on the probe light wavelength. The total reflectivity can be written as:

$$R = R_0 + \Delta R \tag{2}$$

where R_0 is the reflectivity signal at room temperature and ΔR is the reflectivity variation due to temperature variation:

$$\Delta R = \Delta R_0 + \Delta R_f \cos(2\pi f t + \varphi) + \textit{higher frequency terms} \tag{3}$$

with ΔR_0 the DC reflectivity variation due to the DC dissipated power, ΔR_f the reflectivity variation due to the dissipated power at frequency f, φ the thermal phase shift at frequency f. "higher frequency terms" includes all the reflectivity variations due to the dissipated power at harmonics 2f, 3f… Since the power is mainly dissipated at frequency f, we measure $\Delta R_f/R$ to evaluate the ΔT_f temperature variation at frequency f.

Among thermal mapping methods, thermoreflectance [8], [9] is an accurate, spatially resolved, non-contact and non-invasive method. The reflectivity variation implies an intensity variation of the light reflected to the photodetector. Thus, measuring the relative variation of detector photocurrent ΔI/I, we deduce $\Delta R_f/R$ and then ΔT_f if κ is known. The set-up is presented in fig.2. The probe laser beam first crosses a Faraday isolator coupled to a half wave plate to eliminate a possible probe laser signal coming back into the laser cavity and to adjust the laser intensity. Then, it is separated into a reference beam and a probe beam using a polarizing beam splitter (PBS). The probe beam is then focused on the sample surface through a ×40 magnitude microscope objective. After reflection, the probe beam is transmitted towards the detection arm by a second PBS and focused on the differential detector. A removable mirror sends the reflected probe and the light coming from a white lamp to a CCD camera to visualize the probe position on the sample surface. A dichroic mirror prevents the diode signal from back reflections inside the probe laser cavity. In addition, a 980nm notch filter and two 632nm interferential filters are used so that only the probe wavelength could be transmitted to the differential detector. This detector eliminates the DC component dominating the reflected signal, the reference signal input being adjusted by a half wave plate to compensate the DC reflected signal. Then the differential signal is measured by a lock-in amplifier locked at f to extract ΔR_f. We also measure the total reflectivity R to deduce $\Delta R_f/R = \kappa \Delta T_f$. The differential detector also enables to avoid a possible lock-in amplifier input saturation and to eliminate possible experimental noise sources affecting both reference and reflected beams. Subsequently, $\Delta R_f/R$ is simply noted ΔR/R.

Since κ is wavelength dependent, we had first compared the TR signal measured on the diode facet for different laser probe wavelengths, namely 408, 532, 632 and 835nm. The maximum signal had been obtained for the 632nm wavelength. Subsequently, a He-Ne laser was chosen as a probe for all the measurements presented. The spot diameter was evaluated to 3μm approximately and the ΔR/R set-up sensitivity was measured to be as low as 2×10^{-6}.

III. Temperature Variation Measurements

The measurements are done on 3 laser diodes of each type, and for each one, they are repeated three times. The results are the mean values obtained on each kind of diodes. To evaluate the UPW length influence on the output facet temperature variation, we first measured the TR signal along the y axis when I_{max}=800mA (fig.3). The first point (taken as y=0) is just under the emitting source towards the AlN heat sink. The displacement step is 2μm on the first 10μm and then 5μm between y=10μm and 80μm. Close to the source (from y=0 to 5μm), the S-UPW diode is heating more than the L-UPW one, with a difference reaching almost 40% for y=0. Then, beyond 5μm, the L-UPW diode heats more than the S-UPW one from 20% at y=6μm down to less than 10% at 80μm. The maximum ΔR/R measured at y=0 was ($4.160\times10^{-3}\pm2\times10^{-6}$) and ($2.680\times10^{-3}\pm2\times10^{-6}$) for the S-UPW and L-UPW diodes respectively. The uncertainty corresponds to the repeatability error. Other measurements, made along the black horizontal full line, for y=5μm and between x=-20μm and x=20μm, confirmed that on the active region and in its close vicinity (closer than 5 μm), the S-UPW laser diode heats more by 20% than the L-UPW laser diode, in accordance with simulation results [4]. On the contrary, when moving away from the active zone, the S-UPW diode signal becomes lower than the L-UPW diode one with a 10% difference. The thermal power seems then to be dissipated differently: for the S-UPW diodes, the heating

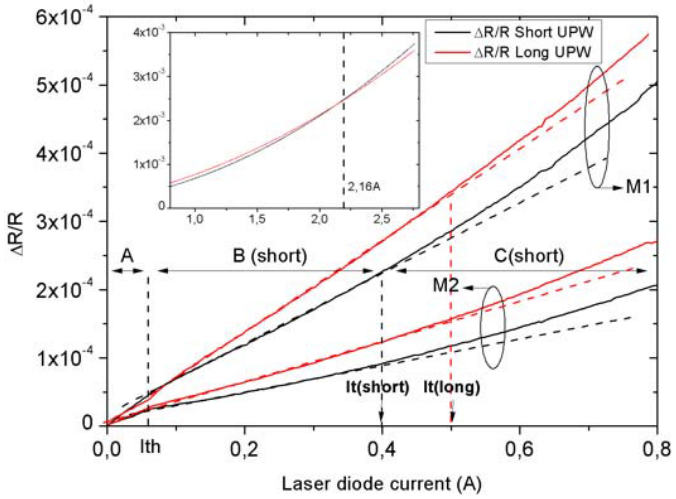

Fig. 4. ΔR/R signal for two positions (M_1 and M_2). Zones B and C correspond to the short UPW diode. Dashed lines correspond to the linear fit between I_{th} and I_t. Inset: extrapolation for high currents.

is more concentrated on the active region whereas, for the L-UPW diodes, it spreads on the whole facet, being more homogeneously distributed.

Then, we particularly focused on two particular positions: one close (10μm) to the emitting source (M_1) and one 60μm far from it (M_2) as indicated in fig.1. For each position, we measured the TR signal as a function of the current, I_{max} varying from 6mA to 800mA with a 3mA step (fig.4). We distinguish three zones. The first one (zone A), under the threshold, has a linear behavior with a slope α_1. Then, between the threshold and a transition current I_t (zone B), the behavior is still linear but with a different slope α_2. Finally, in the last zone C beyond I_t, the behavior appears non-linear. This can result in a fast and strong temperature increase and then in a COD at very high current.

From a thermal point of view, three contributions can be considered in the facet temperature variation [10]. The first one is due to the conversion of the electrical power into heat and is the only active contribution under the threshold. Starting above the laser threshold, part of the input electrical power is extracted as optical output thus reducing the temperature slope: this is the second contribution. The last contribution comes from the surface heat source which creates a new temperature increase and can lead to a huge thermal runaway rapidly inducing a COD since it is concentrated on the emission area and its amplitude strongly increases with the current. This last contribution is then negligible at low current (A and B zones) and far from the active region (at M_2). But when approaching the active region at M_1, it becomes dominant, even at relatively low current (zone B), and can compensate the second contribution, finally leading to a temperature increase in zone B. The α_2/α_1 ratio is then an indicator of the facet heating.

For position M_2, as expected, α_2/α_1 is smaller than 1 since a part of the electrical power injected is converted into light and hence the proportion of the electrical power converted into heat decreases. Then, in zone C, the TR signal increases faster because of the surface source whose amplitude strongly increases with the supplied current. At this position, the L-UPW diode heats more than the S-UPW one, in agreement with fig.3. For position M_1, the L-UPW diode still heats more than the S-UPW one. When moving from M_2 to M_1, the α_2/α_1 ratio increases from 0.54 to 0.7 for the S-UPW diode and from 0.67 to 1.18 for the L-UPW one. Hence, for both kinds of diodes, when approaching the emitting zone, the surface source contribution increases but, in the last case (L-UPW at position M_1), the surface source contribution is clearly dominating, which is consistent with the previous results showing that beyond 5μm from the source, the L-UPW diode heats more than the other one.

To determine which UPW will be more sensitive to COD, the non-linear behavior needs to be analyzed in detail since COD will occur at very high current well beyond 800mA, i.e. far away in the non-linear zone C. The I_t current, indicating the onset of the non-linear behavior (which leads to thermal runaway), is evaluated to 500mA for the L-UPW diode but only 400mA for the S-UPW diode (fig.4), hence 20% lower. In addition, we fitted the curves by a polynomial fit in the I_t-0.8A range and extrapolated them at very high current up to 2.75A (inset in fig.4). We then observe that the non-linearity is higher for the S-UPW: the quadratic term is 4.2×10^{-4} and 3.3×10^{-4} for the S-UPW and L-UPW respectively. As a result, for very high current beyond 2.16A, the S-UPW diode heats more than the L-UPW counterpart. The thermal runaway will then be triggered at lower current. We confirm it measuring the optical power as a function of the current until the COD arises. It occurred at 2.65A for the S-UPW diode whereas for the L-UPW one, the COD was not yet reached at 3A.

All the measurements lead to the conclusion that the L- UPW diode heats a little bit more than the S-UPW one for low currents and far from the source (beyond 5μm from it). However, the temperature variation is much higher (up to 40%) for the S-UPW diodes in the source close vicinity and at high currents. In addition, for currents above I_t, the temperature variation becomes non-linear for both kinds of diodes but it increases more rapidly for the short UPW diode. These S-UPW diodes may then be less reliable at very high current and should be more sensitive to COD.

Other papers have studied the influence of unpumped windows on laser diode reliability, either by simulation [4] or experimentally [3], [11]. In [11], Ohgog and al studied the effect of a current blocking region on the light output power and on the driving current. In [3], Rinner uses μ-Raman spectroscopy to evaluate the facet and averaged waveguide temperatures. It is quite difficult to compare their results with ours because, concerning Ohgoh, the laser diode structure he studied is very different. As for Rinner, he shows a reduction of the facet overheating due to the unpumped window much larger than the one we have measured. One of the possible explanations might be that the measurements are not performed at the same position since we have measured under the emitting zone while he has investigated directly on it. Moreover, μ-Raman measurements reported large uncertainties (up to $\pm$50%) [3], [6]. Nevertheless, all these studies lead to the same conclusion that a long unpumped window improves the laser diode reliability, especially by increasing the COD threshold. Our study confirms these results but also

shows for the first time and with a very good accuracy, how the thermoreflectance signal, hence the temperature variation, is spatially distributed on the output facet.

REFERENCES

[1] M. Fukuda, M. Okayasu, J. Temmyo, and J. Nakand, "Degradation behavior of 0.98-μm strained quantum well InGaAs/AlGaAs lasers under high-power operation," *IEEE J. Quantum Electron.*, vol. 30, no. 2, pp. 471–476, Feb. 1994.

[2] H. Horie, Y. Yamamoto, N. Arai, and H. Ohta, "Thermal rollover characteristics up to 150 °C of buried-stripe type 980-nm laser diodes with a current injection window delineated by a SiN_x layer," *IEEE Photon. Technol. Lett.*, vol. 12, no. 1, pp. 13–15, Jan. 2000.

[3] F. Rinner *et al.*, "Facet temperature reduction by a current blocking layer at the front facets of high-power InGaAs/AlGaAs lasers," *J. Appl. Phys.*, vol. 93, no. 3, pp. 1848–1850, 2003.

[4] X. Liu, M. H. Hu, C. G. Caneau, R. Bhat, and C.-E. Zah, "Thermal management strategies for high power semiconductor pump lasers," *IEEE Trans. Compon. Packag. Technol.*, vol. 29, no. 2, pp. 268–276, Jun. 2006.

[5] P. E. Raad, P. L. Komarov, and M. A. Bettiati, "Thermoreflectance measurements for optically emitting devices," in *Proc. 18th Int. Workshop THERMINIC*, Budapest, Hungary, Sep. 2012, pp. 1–3.

[6] M. Hempel, J. W. Tomm, T. Elsaesser, and M. Bettiati, "High single-spatial-mode pulsed power from 980 nm emitting diode lasers," *Appl. Phys. Lett.*, vol. 101, no. 19, pp. 191105-1–191105-5, 2012.

[7] M. A. Bettiati, "High optical strength GaAs-based laser structures," *Microelectron. Rel.*, vol. 53, nos. 9–11, pp. 1496–1500, 2013.

[8] S. Dilhaire, S. Grauby, and W. Claeys, "Thermoreflectance calibration procedure on a laser diode: Application to catastrophic optical facet damage analysis," *IEEE Electron Device Lett.*, vol. 26, no. 7, pp. 461–463, Jul. 2005.

[9] P. W. Epperlein, "Mapping of local temperatures on mirrors of GaAs/AlGaAs laser diodes," *Inst. Phys. Conf. Ser.*, vol. 112, chapter 8, pp. 633–638, 1990.

[10] S. Dilhaire, S. Grauby, S. Jorez, L.-D. P. Lopez, E. Schaub, and W. Claeys, "Laser diode COFD analysis by thermoreflectance microscopy," *Microelectron. Rel.*, vol. 41, nos. 9–10, pp. 1597–1601, 2001.

[11] T. Ohgoh, T. Fukunaga, and T. Hayakawa, "Technologies and applications of Al-free high-power laser diodes," *Elect. Eng. Jpn.*, vol. 158, no. 1, pp. 53–59, 2007.